Journal of Alloys and Compounds 577 (2013) 283–287

Contents lists available at SciVerse ScienceDirect

Journal of Alloys and Compounds

journal homepage: www.elsevier.com/locate/jalcom

Evolution of visible photoluminescence of Si quantum dots embedded in silicon oxide matrix

Anna Yu. Karlash [a,*], Valeriy A. Skryshevsky [a], Gennady V. Kuznetsov [a], Vasyl P. Kladko [b]

[a] Institute of High Technologies, Taras Shevchenko National University of Kyiv, 64/13 Volodymyrska str., Kyiv 01601, Ukraine
[b] Lashkaryov Institute of Semiconductor Physics, National Academy of Sciences of Ukraine, 41, pr. Nauki, Kyiv 03028, Ukraine

ARTICLE INFO

Article history:
Received 6 July 2012
Received in revised form 3 May 2013
Accepted 7 May 2013
Available online 22 May 2013

Keywords:
Nanostructured composite materials
Silicon quantum dots
Photoluminescence

ABSTRACT

Photoluminescence properties of nc-Si/SiO_x nanocomposites produced by pressing the mixture of the silica aerogel powder with the porous silicon have been studied. The transformation of emission spectra of Si quantum dots, its quantum yield and emission kinetics during the long time (few months) aging in ambient conditions and formation conditions (external pressure) were observed. The different behavior of short and long wave range emission of Si quantum dots embedded in silicon oxide matrix has been obtained. The observed blue-shifting (from 2.02 to 2.05 eV) of emission peak associated with the free exciton recombination in Si quantum dots at forming pressure increasing is explained by the reduction of average Si quantum dot dimension due to the breaking away the surface irregularities and smoothing of the Si nanoparticles surface. Effect of a strong increase in intensity (more than 1 order) and blue shifting of emission of Si quantum dots were discovered in nc-Si/SiO_x nanocomposites at few months' storage in ambient conditions. Such effects were explained in terms of both surface passivation and the carrier confinement. It was also confirmed by the fact that for aged composites the photoluminescence kinetics transforms by adding the stretched exponential term to the single exponential low.

1. Introduction

It is well known that the electrochemical etching of moderate doped silicon results in porous silicon (PS) formation which reveals the strong photoluminescence (PL) in visible region. The estimation showed that PL quantum yield can achieve more than 20% [1] and the electroluminescence with much lower quantum yield was observed too [2]. It seemed the all-silicon optoelectronics becomes a reality due to creation of the light emitting PS structures while today the efficient silicon photodetectors production is rather technological task than the research subject. However, the PS have been observed to degrade during aging in ambient atmosphere or under UV illumination due to progressive oxidation of its large internal surface [3,4]. The growth of native oxide also induces a shift in emission energy [5]. Passivation of PS is absolutely necessary to prevent competitive non-radiative recombinations (e.g. trapping by surface states) and the PL degradation owing to chemical evolution of PS surface. Different approaches have been proposed in order to stabilize the PS and nc-Si luminescence: Si ion implantation into SiO_2 substrate [6], LPCVD deposition of non-stoichiometric SiO_x ($1 < x < 2$) with subsequent thermal annealing precipitation [7,8], magnetron sputtering technique [9], surface modification and covering of PS surface [10–13]. The creation of nc-Si/SiO_x nanocomposites by different methods [9,14–16] allowed obtaining Si nanoparticles embedded into the dielectric envelope preventing the oxidation processes. The stabilization of Si surface was achieved also at preparation of colloidal solution of Si nanoparticles in organic solutions [17,18].

Different composites materials have been used like phosphorescent materials, photodetectors, catalysts, waveguides, lasers and sensors [19–21]. There has been recent interest in the study of the properties of silica aerogel powders [22] and silica aerogel – nc-Si composites that also demonstrate intense luminescence in the visible region [23–25]. In this work we have investigated the evolution of PL spectra of nc-Si/SiO_x nanocomposites as prepared and after aging at ambient conditions. Nanocomposites were produced by pressing the mixture of the silica aerogel powder with the PS powder into pellets as was proposed in our earlier work [23].

2. Materials and methods

The silica aerogel preparation method was based on the gradual water removing from the silicon acid gel. The silica gel, prepared from the sodium silicate water solution, was converted into an aerogel by a supercritical drying process [26]. PS or nc-Si powder was produced by electrochemical etching of p-Si wafers in $HF:C_2H_5OH:H_2O$ electrolyte at constant current mode of 50 $mAcm^{-2}$ during 2.5 h. Porous powder was then rinsed in ethanol, dried in air and thoroughly grated.

* Corresponding author. Tel./fax: +380 445260582.
E-mail address: anna_karlash@ukr.net (A.Yu. Karlash).

0925-8388/$ - see front matter © 2013 Elsevier B.V. All rights reserved.
http://dx.doi.org/10.1016/j.jallcom.2013.05.031

The samples used for PL measurements were prepared by mixing the silica aerogel powder with the PS powder in a composition 98:2 and pressing into pellets with diameter of about 12 mm and typical thickness of 0.2–0.3 mm at different pressures (10.7, 13.3 and 16 MPa). The optical investigations were performed of as prepared samples and those after aging in ambient atmosphere for 7, 14, 30 and 60 days.

The XRD spectra were recorded in the 2θ range from 10° to 70° at a scan rate of 0.022°/s in the Bragg–Brentano geometry using a X'Pert PRO MRD X-ray difractometer (Holland). The XRD patterns were analyzed to investigate the crystallinity and the orientation of the silicon crystalline plane in samples.

The temporal domain PL spectra were measured at the room temperature using the time correlated single photon counting technique (TCSPC) [10]. The samples were excited with nitrogen laser pulses at 337 nm (3.68 eV), repetition rate 100 Hz, pulse duration τ = 8 ns and average power 20 mW. The beam was focused onto the samples surface with diameter of 2–3 mm approximately, the stray light was perfectly rejected and the special optical filter was used to avoid the influence of dispersive laser irradiation on resulting PL spectra. The proper emission band was selected by a monochromator (MS2004, SOLAR TII) and registered by a combination of photomultiplier (HAMAMATSU C6270) and analog-to-digital board (up to 1 GHz sample rate). For the improvement of signal-to-noise ratio an accumulation and averaging were produced over 50 spectra.

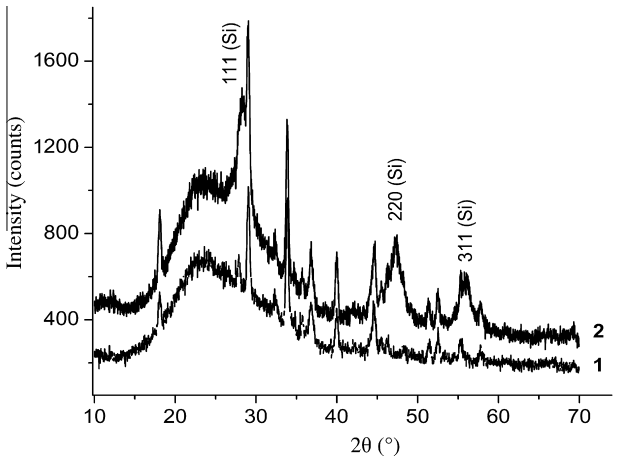

Fig. 2. XRD spectra of the pressed SiO_x (1) and nc-Si/SiO_x (2) nanoconposites.

3. Results and discussion

Fig. 1a presents the TEM image of nc-Si suspension in colloidal solution performed in our previous works [17,18]. The TEM analysis showed nc-Si grains to have the quasi-spherical shape, each quasi-sphere is studded with holes and hillocks which give clear and dark spots on the TEM image (Fig. 1a). In general, their shape was already described in terms of fractal geometry [27]. The initial nc-Si powder consists of large (>10 nm) and numerous small denser (<5 nm) crystallites, Fig. 1b presents the histogram of small nanocrystals size distribution.

Fig. 2 shows the XRD patterns of silica aerogel (1) and nc-Si/SiO_x nanocomposite (2) pressed at 16 MPa. All samples show intense numerical diffraction peaks of cristobalite and quartz (SiO_2). The appearance of broadened diffraction peak at 25° suggests that the aerogel matrix has a combined amorphous and crystalline structure. The XRD spectrum of nc-Si/SiO_x nanoconposite reveals diffraction peaks of Si (111), (220) and (311) planes at 2θ angles of 28.4°, 47.3° and 56.4° respectively.

The average Si crystallite sizes D_{XRD} were roughly estimated from these diffraction peaks using the Sherrer equation, the wide size distribution was revealed in the range <9 nm. The sizes of nc-Si in the TEM image in Fig. 1a are of the same order as the sizes determined from XRD measurements.

Fig. 3a shows the evolution of the integrated PL spectra of freshly prepared samples with the pressure increasing.

The PL spectra were observed to have the complex structure with stipulated peaks at around 1.8 eV and 2.1 eV. The best approximation of experimental results were done by decomposition of the PL spectra on to 3 Gaussian components with maxima at 1.87, 1.97 and 2.02 eV, as one can see on Fig. 3a. The Gaussian peak positions as well as FWHM at different pressures are presented in Fig. 3b. The low-energy peak at 1.87 eV does not change its position, as well as its FWHM of 0.1 eV, with the pressure increasing. By contrary, short wavelength peaks at 1.97 and 2.02 eV demonstrate the blue-shift by 0.05 eV with the small increasing of FWHM.

Such behavior of emission spectra at pressure increasing can be explained in a following way. Firstly, as it was showed in our previous work [23], the pure silica aerogel reveals the broad PL spectra in visible region with the intense peaks at 3.26, 3.02 and 2.53 eV and more weak peak at 2.18 eV. As can be seen from Fig. 3a, even intense PL peaks attributed to SiO_x matrix do not observed. So, the contribution of aerogel emission to observed spectra (Fig. 3a) has been neglected and the PL has been attributed to the emission of nc-Si.

Despite of the existence of a lot nc-Si emission models, the weight of evidence now clearly shows that only quantum confinement based models are consistent with the experimental data as a whole [28]. The light absorption occurs in quantum confined structures, but radiative recombination involves localized surface states [29]. Either the electron or the hole or both of them can be localized and the PL emission arises with participation of surface states or via the free exciton recombination (see Fig. 4c, channels 2, 3 and channel 1, correspondingly). Hence, a hierarchy of transitions is possible which explains the various emission bands of nc-Si. The energy difference between absorption and emission peaks is well explained in this model, because photoexcited carriers relax into

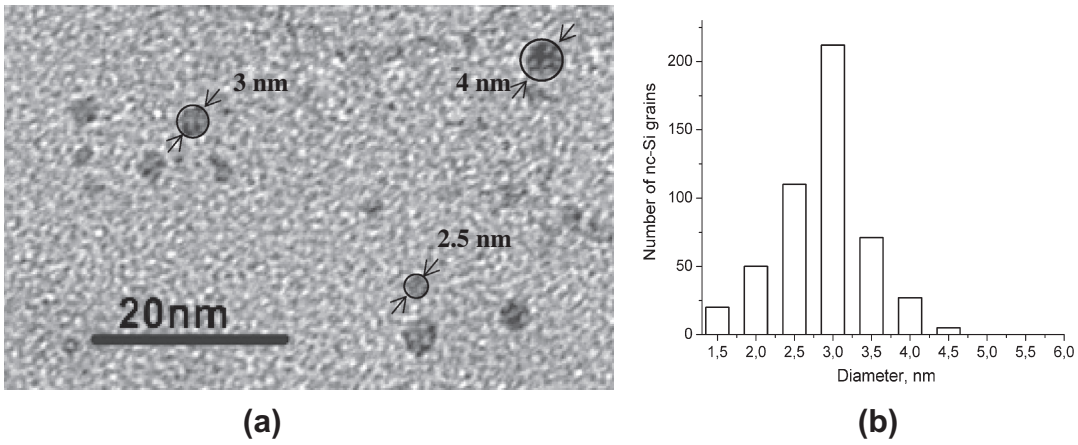

Fig. 1. (a) TEM image of Si nanoparticles constituting the nanopowder suspension into the colloidal solution [18] and (b) histogram of Si nanocrystal size distribution.

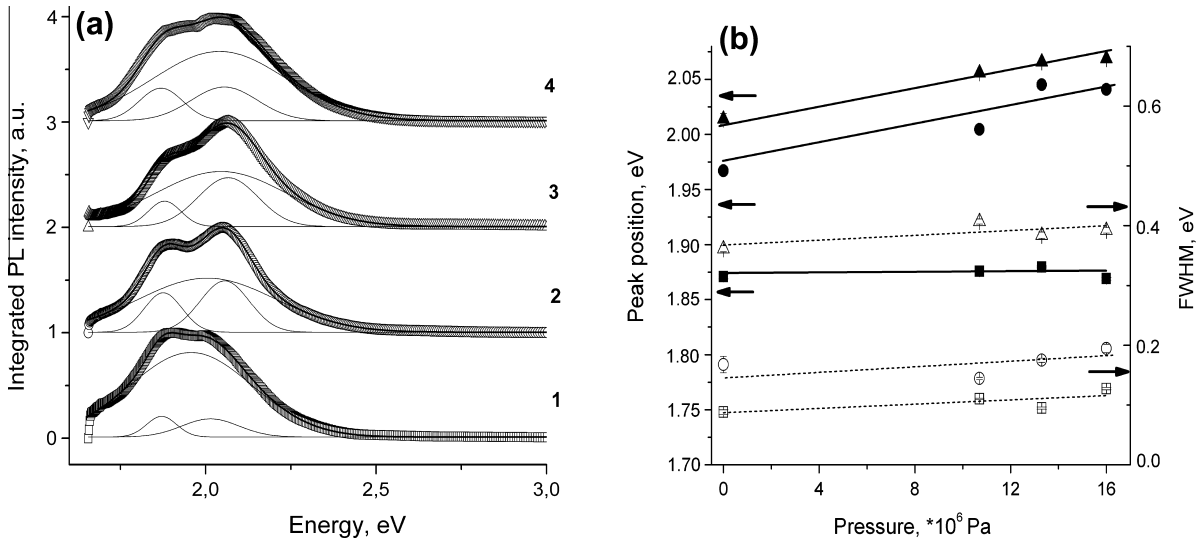

Fig. 3. (a) Integrated PL spectra of freshly prepared nc-Si/SiO_x samples: 1 – nc-Si/SiO_x powder, nc-Si/SiO_x nanocomposites pressed under: 2 – 4 t, 3 – 5 t and 4 – 6 t and (b) Gaussian peak positions (filled symbols, the left-hand *y*-axis) and FWHM (open symbols, the right-hand *y*-axis) of freshly prepared samples.

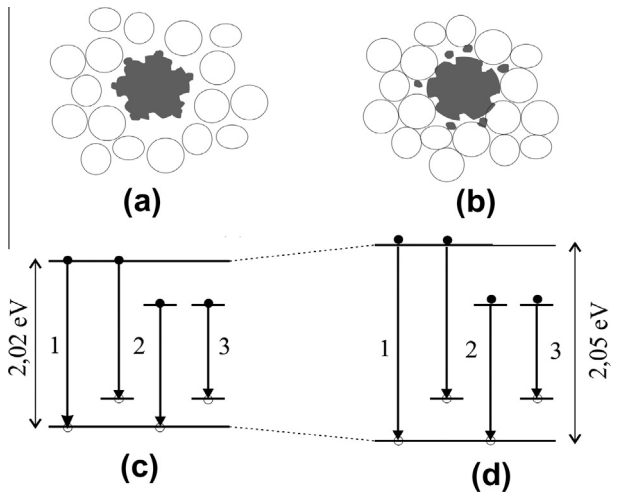

Fig. 4. Model of fractal-type nc- Si in powder (a) and in pressed nanocomposite (b) (for simplicity SiO_x particles are depicted as opened spheres). Schema of exciton recombination in free Si quantum dot (c) and Si quantum dot embedded in SiO_x matrix (d).

surface states. The existence of surface states in nc-Si was proved by different methods: from the steady-state *I–V* and high frequency *C–V* measurements [30], analysis of *I–V* curves in the space–charge-limited current mode [31], the deep-level transient spectroscopy [32] and thermally stimulated currents [33]. If we will consider the nc-Si as crystalline quantum dots, the high-energy emission peak at 2.02 eV could be attributed to the free exciton recombination and its energy is close to band gap of quantum dots. This energy corresponds to spherical silicon quantum dot of 3.0 nm diameter [19,34,35].

For analysis we took into consideration the data of Transmission Electron Microscopy (TEM) of Si nanoclusters (Fig. 1a). Fig. 4a and b represents the fractal-type model of Si quantum dot in SiO_x powder and after compaction into pellet by mechanical pressing. In this case the surface roughness becomes comparable to the nanocrystallites dimension. The fractal character of the specific surface should be taken into account when an interaction of nc-Si with fluids is occurred (for example, at auto filtration effect, when small Si nanoparticles pass through mesoporous silicon membrane (so-called, silicon-by-silicon filtration) or size selection at application of centrifugation technique [17,18]. By analogy with these fluid methods of nc-Si size selection, the pressing of nc-Si and aerogel mixture results in breaking away the surface irregularities and smoothing of the nc-Si shape. Then the shift of band gap from 2.02 to 2.05 eV is due to the reduction of average nc-Si dimension (Fig. 3d).

At that time, there is no evidence of the low-energy peak shifting with the pressure increasing (Fig. 3b). We can consider that the peak at 1.87 eV is related to the recombination of excitons localized on deep surface states (deep level surface states may not be tied to the edge of one of the allowed bands). Peak at 1.97 eV can be due to the emission with participation of surface states via channel 2 (free electron and a hole trapped on surface state or trapped electron and free hole). Note, that the existence of Si size distribution is also confirmed by large value of FWHM for all PL peaks.

The dependence of PL from external factors (external pressure) or from the variation of the nc-Si chemistry (oxidation) is naturally accounted for by surface states changes [29] and size reduction. Indeed, the same effect of nanocomposite spectra evolution is observed during the aging in ambient atmosphere. Fig. 5a demonstrates the PL spectra of the nc-Si/SiO_x sample pressed at 16 MPa as prepared and aged during 1 and 2 months. The PL peak intensity increases by 6 times at 1 month aging and more than 10 times at 2 months aging. At the same time the blue-shift behavior of two high energy peaks with their soft broadening and no significant change at aging prolongation have been observed (Fig. 5b).

Such PL behavior is typical for nc-Si: keeping in ambient air results in emission blue shifting, however, the PL intensity was observed both to increase and decrease [36–38]. Such effects are explained in terms of surface passivation and carrier confinement. The similar result was obtained in [37] for Si nanoparticles, the PL maximum of nanoparticles with diameters between 2 and 5 nm after exposure to air shifts to higher energies while its intensity and FWHM both increase with the time. In our case the blue-shift of high-energy PL peaks is stipulated by the presence of oxide matrix. Among reasons we can note the subsequent nc-Si oxidation due to both solid–solid interaction with hydroxyl terminated silica aerogel (the last is very clearly detected in FTIR spectra of aerogel [23]) and reactions with atmospheric oxygen and water:

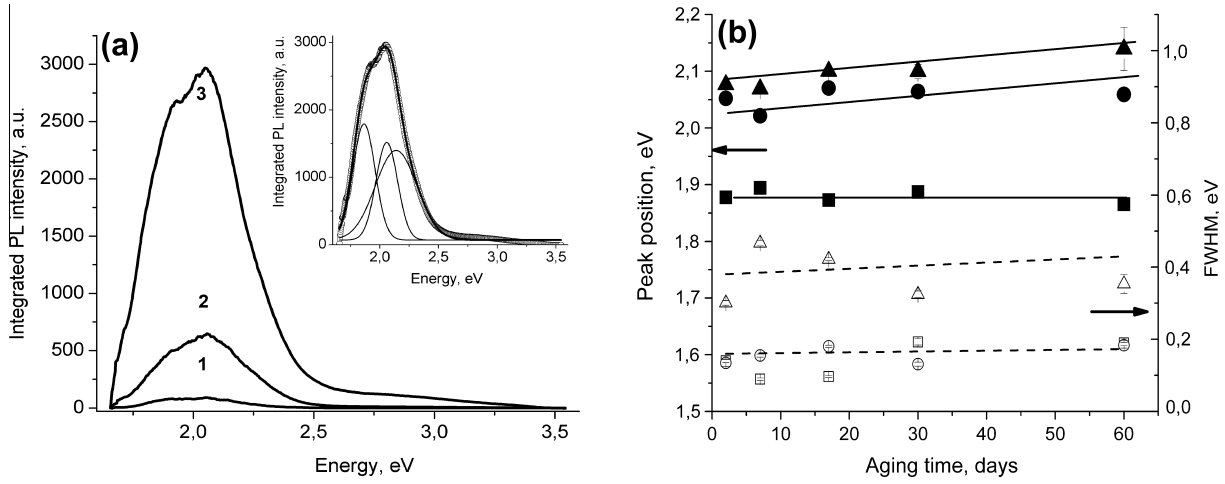

Fig. 5. (a) The integrated PL spectra of nc-Si /SiO_x nanocomposite pressed at 6 ton: freshly prepared (1) and after 30 days (2) and 60 days (3) aging, inset shows Gaussian peak decomposition of the sample aged during 60 days; (b) The corresponding PL Gaussian peak positions and FWHM.

$Si + O_2 \rightarrow SiO_2$ or $Si + 2H_2O \rightarrow SiO_2 + H_2$. We suppose that process of nc-Si oxidation may be accompanied by suppressing of non-radiative recombination channels.

Fig. 6 shows the normalized PL decay curves measured at 660 nm (1.88 eV) for nc-Si/SiO_x sample pressed at 16 MPa freshly prepared and after 30 and 60 days aging in ambient atmosphere. The PL kinetics of freshly prepared samples (Fig. 6, curve 1) follows the simple exponential decay law. The experimental data can be satisfactory fitted by a single-exponential decay with decay time τ. The character of PL decay kinetics drastically changes during storage at ambient conditions since for aged samples the dependence $I(t)$ is described by adding the stretched exponential term to the single exponential decay: $I(t) = A_1\exp\{-(t/\tau_1)^{\beta}\} + A_2\exp(-t/\tau_2)$, were β is the dispersion factor [39], τ_1 and τ_2 – characteristic decay times (inset on Fig. 6).

Table 1 presents the calculated values of PL decay time and dispersion factor β for studied samples obtained from PL decay curves recorded at 660 nm. The prolongation of storage time results in increasing of decay times τ_1 and τ_2. Simultaneously the dispersion factor decreases from 1.0 to 0.78–0.82.

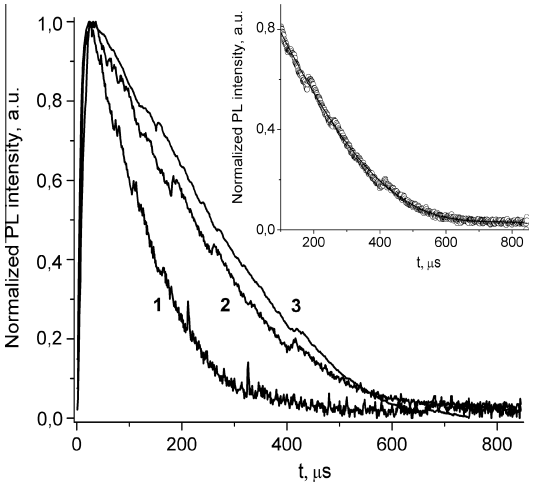

Fig. 6. Normalized PL decay curves measured at 660 nm for the nc-Si/SiO_x sample pressed at 6 ton: (1) freshly prepared and after (2) – 30 and (3) – 60 days aging. Inset shows the best-fitting of the PL decay curve for nc-Si/SiO_x composite after 30 days aging.

Table 1
The calculated values of PL lifetimes and dispersion factor β.

Sample	PL lifetimes, τ_1/τ_2 (μs)			Dispersion factor β		
	Fresh	1 Month aging	2 Months aging	Fresh	1 Month aging	2 Months aging
SiO_2/nc-Si (4 t)	–/100.2	209.0/223.0	267.5/311.7	1	0.92	0.82
SiO_2/nc-Si (5 t)	–/116.9	157.7/173.1	286.5/326.2	1	0.92	0.78
SiO_2/nc-Si (6 t)	–/105.9	174.5/181.6	355.7/302.0	1	0.9	0.8

Table 1 The calculated values of PL decay times and dispersion factor β for nc-Si/SiO_x nanocomposites freshly prepared and aged in ambient conditions.

It was pointed out that the some disorder in the materials plays a key role producing the stretched-exponential PL decay [40–42]. The disorder of materials that impacts on PL decay time can be in the form of (i) a wide distribution of the Si nanocrystals size, (ii) a random spatial arrangement of the nanocrystals and (iii) the structure of the nanocrystal surfaces [41]. The values of $\beta < 1$ in the stretched-exponential kinetics correspond to the existence of a broad distribution of lifetimes which describes the elementary relaxation processes, either radiative or nonradiative. As a rough approximation the stretched-exponential decay with $\beta < 1$ can be considered as superposition of many exponential decays. Moreover, the presence of retrapping states in energy gap with no inherent necessity to have a disorder in the sample also provides the stretched-exponential low [43]. If consider that the dispersion factor β is associated with the density of trap states, the decreasing of β during sample aging could means the increasing of the interfacial nc-Si/SiO_x retraping states amount, that are responsible for radiative recombination.

5. Conclusions

In this work we have investigated the evolution of PL spectra of nc-Si/SiO_x nanocomposites as prepared and after aging at ambient conditions. Nanocomposites were produced by pressing the mixture of the PS and silica aerogel powders.

The PL spectra were observed to have the complex structure with stipulated peaks at 1.87, 1.97 and 2.02 eV associated with exciton recombination in Si quantum dots. The blue-shift behavior

of the PL spectra with the pressure increasing has been observed for freshly prepared samples. The pressing of Si quantum dots and aerogel mixture results in breaking away the surface irregularities and smoothing of the Si surface. Then the shift of band gap from 2.02 to 2.05 eV under pressure increased to 6 tons occurs due to the reduction of average Si quantum dot dimension. Effect of a strong increase in intensity (more than 1 order) and blue shifting of Si quantum dots emission are discovered in nc-Si/SiO_x nanocomposites at few months' storage at ambient conditions. Such effects can be explained in terms of both surface passivation and the carrier confinement at partial oxidation of Si quantum dots. It confirmed by the fact that for aged composites the PL kinetics transforms by adding the stretched exponential term to the single exponential low. If PL freshly prepared samples is fitted by a single-exponential decay with decay time τ, for aged samples the dependence $I(t)$ is described by adding the stretched exponential term to the single exponential decay: $I(t) = A_1\exp\{-(t/\tau_1)^{\beta}\}+A_2\exp(-t/\tau_2)$. The prolongation of storage time has been observed to result in increasing of PL decay times τ_1 and τ_2 as well as decreasing of dispersion factor β. The decreasing of dispersion factor during sample aging means the increasing of the interfacial retrapping states amount that are responsible for radiative recombination as a result the PL quantum yield increases, the PL decay times increase due to suppressing of nonradiative recombination in this system at the passivation of the nc-Si/SiO_x interface.

References

[1] B. Gelloz, A. Kojima, N. Koshida, Appl. Phys. Lett. 87 (2005) 031107.
[2] B. Gelloz, N. Koshida, Jpn. J. Appl. Phys. Part 1 43 (4B) (2004) 1981–1985.
[3] A.S. Len'shin, V.M. Kashkarov, S.Yu. Turishchev, M.S. Smirnov, E.P. Domashevskaya, Tech. Phys. Lett. 37 (2011) 789–792.
[4] V.A. Skryshevsky, Appl. Surf. Sci. 157 (2000) 145–150.
[5] Tevhit. Karacali, Bulent. Cakmak, Hasan. Efeoglu, Opt. Exp. 11 (2003) 1237–1242.
[6] Tsutomu. Shimizu-Iwayama, Norihiro. Kurumado, David.E. Hole, Peter.D. Townsend, J. Appl. Phys. 83 (1998) 6018–6022.
[7] T. Baron, F. Martin, P. Mur, J. Cryst. Growth 209 (2000) 1004.
[8] Goh Boon Tong, Muhamad Rasat Muhamad, Saadah Abdul Rahman, Opt. Mater. 34 (8) (2012) 1282–1288.
[9] P. Aliberti, S.K. Shrestha, Ruoyu Li, M.A. Green, G.J. Conibeer, J. Cryst. Growth 327 (1) (2011) 84–88.
[10] Be. Benyahia, N. Gabouze, M. Haddadi, L. Guerbous, K. Beldjilali, Thin Solid Films 516 (2008) 8707–8711.
[11] A. Benilov, I. Gavrilchenko, I. Benilova, V. Skryshevsky, M. Cabrera, Sensors Autat. A 137 (2007) 345–349.
[12] B. Gelloz, N. Koshida, J. Appl. Phys. 98 (2005) 123509.
[13] J.L. Gole, J.A. DeVincentis, L. Seals, P.T. Lillehei, S.M. Prokes, D.A. Dixon, Phys. Rev. B 61 (2000) 5615.
[14] Y.Q. Wang, G.L. Kong, W.D. Chen, H.W. Diao, C.Y. Chen, S.B. Zhang, X.B. Liao, Appl. Phys. Lett. 81 (2002) 417–441.
[15] B. Garrido, M. Lopez, C. Garcia, J. Appl. Phys 91 (2002) 798.
[16] R.J. Walters, J. Kalkman, A. Polman, H.A. Atwater, M.J.A. de Dood, Phys. Rev. B 73 (2006) 132302.
[17] V. Lysenko, V. Onyskevych, O. Marty, V.A. Skryshevsky, Y. Chevolot, C. Bru-Chevallier, Appl. Phys. Lett. 92 (2008) 251910.
[18] T. Serdiuk, V. Lysenko, S. Alekseev, V.A. Skryshevsky, J. Colloid. Interf. Sci. 364 (2011) 65–70.
[19] L. Pavesi, L. Dal Negro, C. Mazzoleni, G. Franzò, F. Priolo, Nature 408 (2000) 440–444.
[20] C.C. Koch, Nanostructured Materials: Processing Properties and Applications, William Andrew Inc., Norwich, NY, 2007.
[21] V.A. Moshnikov, I. Gracheva, A.S. Lenshin, Yu.M. Spivak, M.G. Anchkov, V.V. Kuznetsov, J.M. Olchowik, J. Non-Cryst. Solids 358 (2012) 590–595.
[22] Sun Ki Hong, Mi Young Yoon, Hae Jin Hwang, J. Ceram. Process. Res. 13 (1) (2012) s145–148.
[23] A.Yu. Karlash, Yu.E. Zakharko, V.A. Skryshevsky, A.I. Tsiganova, G.V. Kuznetsov, J. Phys. D: Appl. Phys. 43 (2010) 335405.
[24] J. Amonkosolpan, D. Wolverson, B. Goller, S. Polisski, D. Kovalev, M. Rollings, M.D.W. Grogan, T.A. Birks, Nanoscale Res. Lett. 7 (2012) 397.
[25] E. Borsella, M. Falconieri, S. Botti, S. Martelli, F. Bignoli, L. Costa, S. Grandi, Luigi Sangaletti, B. Allieri, L. Depero, Mater. Sci. Eng. B 79 (2001) 55–62.
[26] M.R. Ayers, A.J. Hunt, J. Non-Cryst. Solids 285 (2001) 123.
[27] T. Nychiporuk, V. Lysenko, D. Barbier, Phys. Rev. B 71 (2005) 115402.
[28] A.G. Cullis, L.T. Canham, P.D.J. Calcott, J. Appl. Phys. 82 (1997) 909–965.
[29] O. Bisi, S. Ossicini, L. Pavesi, Surf. Sci. Rep. 38 (2000) 1–126.
[30] V.A. Vikulov, V.I. Strikha, V.A. Skryshevsky, S.S. Kilchitskaya, E. Souteyrand, J.-R. Martin, J. Phys. D: Appl. Phys. 33 (2000) 1957–1964.
[31] T. Matsumoto, H. Mimura, N. Koshida, Y. Masumoto, J. Appl. Phys. 84 (1998) 6157.
[32] O.V. Tretyak, V.A. Skryshevsky, V.A. Vikulov, Yu.V. Boyko, V.M. Zinchuk, Thin Solid Films 445 (2003) 144–150.
[33] C Anastasiadis, D Triantis, Mater. Sci. Eng B 69–70 (2000) 149–151.
[34] C. Delerue, G. Allan, M. Lanoo, Phys. Rev. B 48 (1993) 11024.
[35] G. Ledoux, J. Gong, F. Huisken, O. Guillois, C. Reynaud, Appl. Phys. Lett. 80 (2002) 4834–4836.
[36] T. Maruyama, S. Ohtani, Appl. Phys. Lett. 65 (1994) 1346.
[37] G. Ledoux, J. Gong, F. Huisken, Appl. Phys. Lett. 79 (2001) 4028–4030.
[38] L.T. Canham, M.R. Houlton, W.J. Leong, C. Pickering, J.M. Keen, J. Appl. Phys. 70 (1991) 422.
[39] M.N. Berberan-Santos, E.N. Bodunov, B. Valeur, Chem. Phys. 315 (2005) 171–182.
[40] Q. Guillois, N. Herlin-Boime, C. Reynaud, G. Ledoux, F. Huisken, J. Appl. Phys. 97 (2004) 3677–3682.
[41] C. Delerue, G. Allan, C. Reynaud, O. Guillois, G. Ledoux, F. Huisken, Phys. Rev. B 73 (2006) 235318.
[42] L. Pavesi, M. Ceschini, Phys. Rev. B 48 (I) (1993) 17625.
[43] R. Chen, J. Lumin. 102–103 (2003) 510–518.